

SIMULATIONS OF 3D SUSPENSION GRAVITY CURRENTS UNDER THE PRESENCE OF A TURBIDITY FENCE

Jaswant SINGH¹, Juichiro AKIYAMA², Mirei SHIGE-EDA³

¹Student member of JSCE, Graduate Student, Dept. of Civil Engineering, Kyushu Institute of Technology
(1-1 Sensui cho, Tobata ku, Kitakyushu 804-8550, Japan)

²Fellow member of JSCE, Ph.D., Professor, Dept of Civil Engineering, Kyushu Institute of Technology

³Member of JSCE, Dr. Eng., Asso. Professor, Dept. of Civil Engineering, Kyushu Institute of Technology.

A 3-D numerical model, which employs the large eddy simulation (LES) and the modified Smagorinsky model, is used to simulate the motion and diffusion of 3D suspension gravity currents under the presence of a turbidity fence. The model constants are determined using the existing data of 2D suspension clouds, and then the validated model is applied for newly obtained experimental results on 3D suspension gravity currents under the presence of a fence. It is confirmed that the model is capable of predicting the complex behavior of the currents to a reasonable accuracy, and the amount of sediments contained within the fence to a good accuracy. In addition, numerical experiments are conducted to demonstrate that the model is a useful tool to examine the placement of a fence to effectively reduce diffusion of turbidity in aquatic environments.

Key Words: *Suspension gravity currents, Turbidity fence, Fluid particle flows, Numerical model.*

1. INTRODUCTION

Large amount of dredge material, soil and rubble is dumped into a body of water for waste disposal, artificial land reclamation projects. Such dumping results in formation of a suspension gravity current over the bottom and causes diffusion of turbidity in wide area. Prediction and control of diffusion of turbidity, therefore, are of particular importance for assessing the impact of such projects on aquatic environments.

To reduce such diffusion of turbidity, a turbidity fence is commonly used. It is usual, however, that the layout and arrangements of the fence have been decided through experiences and/or simple analysis. A logical based method or tool is required to determine the layout and arrangements of the fence.

Numerical prediction of the motion and diffusion of 2D and 3D gravity currents is a matter of serious investigation. For instance, Necker et al.¹⁾ simulated 2D gravity currents in lock-exchange configuration using a 3D numerical model based on spectral-element discretization. Akiyama et al.²⁾ investigated 3D suspension thermals on horizontal bed by using SMAC and MUSCL methods. Huang

et al.³⁾ simulated the evolution of 3D turbidity currents by the κ - ϵ model and reported that turbulent Schmidt number larger than unity provided good match with the experimental data. Ying et al.⁴⁾ investigated the motion of 2D particle clouds produced by direct dumping of sediments into water from the falling to spreading stage by LES. Li and Zang⁵⁾ investigated the motion of 2D and 3D particle clouds based on characteristic based scheme with flux limiters. Singh et al.⁶⁾ simulated 3D gravity currents induced by direct dumping of sediments by LES and reasonable agreement with the experimental data was obtained.

A numerical model may be a best tool for examining the layout and arrangements of the fence, considering the complex behavior of the currents when the fence is presented. From such a point of view, Akiyama et al.⁷⁾ examined the motion and diffusion of the 2D currents with a fence by LES.

This study presents numerical simulations and laboratory experiments on the motion and diffusion of 3D suspension gravity currents under the presence of a fence. The 3D numerical model developed by the authors⁶⁾ is employed and the model parameters, namely, the turbulent Schmidt

number S_{ct} , Smagorinsky constant C_s and a coefficient α for the net deposition rate of sediments are quantified by utilizing the experimental data of the 2D particle clouds reported by Akiyama et al.⁷⁾. Then the validated model is used to simulate 3D suspension gravity currents under the presence of a fence and the results are compared with the newly obtained experimental data. In addition, numerical experiments are conducted taking different heights and placement of a fence to demonstrate that the model is an effective tool to determine the layout and arrangements of a fence.

2. EXPERIMENTS

The experiments were performed in a glass tank (200 cm length, 200 cm width and 75 cm height) by instantaneously releasing a suspension composed of water and glass bead particles from a box. Fig.1 schematically shows the experimental setup and essential parameters used in this study, in which h = ambient water depth, W_0 = total effective gravity force ($=A_0 \times \varepsilon_0 \times g$), A_0 = initial volume of a suspension ($=L \times M \times N$), L , M , N = length, breadth and height, g = acceleration due to gravity, ε_0 = relative excess density of a suspension ($=(\rho_0 - \rho_a)/\rho_a$), ρ_0 = initial density of a suspension, ρ_a = density of ambient water, x_f = intrusion distance of the current, and W_d = effective gravity force per unit area of deposited particles. In this study, $A_0 = 5120 \text{ cm}^3$, initial dimension of a suspension ($L=40\text{cm}$, $M=8\text{cm}$, $N=16\text{cm}$), $\varepsilon_0 = 0.0185$. $W_0=92932 \text{ cm}^4/\text{s}^2$ and $h = 1.25 L$ were chosen. The diameter d and the submerged specific gravity of particle s were 0.0044cm and 1.45, respectively. Placing the fence of height $0.75M$ at a distance of $1.25L$ from the box, and keeping W_0 as $92932 \text{ cm}^4/\text{s}^2$ and the aspect ratio ($=L/M$) as 5, two cases of the fence placement, that is, the fence with opening in the middle (Case 1) and in the corner (Case 2) were considered as shown in Fig.1.

The motion of the currents was recorded simultaneously by three VTR cameras placed one at the top and two in the sides of experimental setup, and was analyzed by PC. Laser slit light was used to visualize the currents. Deposited particles were siphoned from an area of $20\text{cm} \times 20\text{cm}$ shown in Fig.1 after the current was completely seized. The collected particles were dried up and then weighed to calculate effective gravity force W_d . In order to increase the reliability of the experimental results, the experiment was repeated three times under the same condition. The data presented herein are the average of these. The absolute relative error of experimental data for W_d is found to be about 5% of

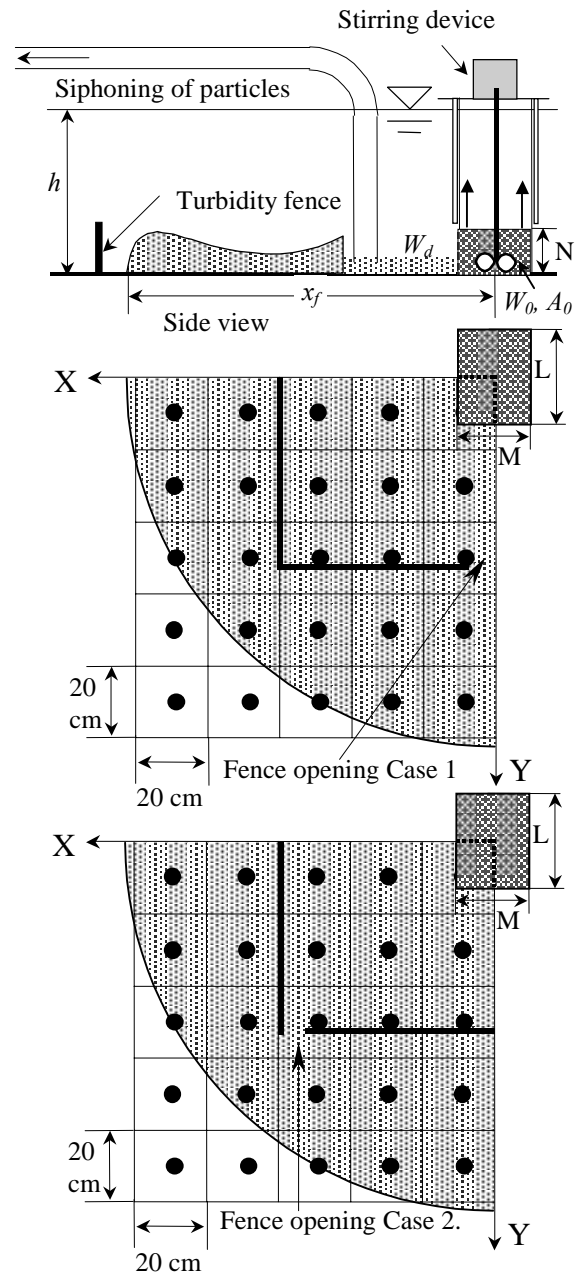


Fig.1 Schematic diagram showing the 3D gravity current and experimental set up.

the average.

3. OUTLINE OF THE MODEL

The details of the model can be referred to Singh et al.⁶⁾, and herein the outline of the model is presented. The model employs one equation Eulerian approach as a solid-fluid two phase flow model, because the Lagrangian approach⁸⁾ is not feasible for suspension gravity currents consisting of the extremely large number of particles. In the modeling, the particle phase is treated as fluid phase and the drift velocity between fluid and particles is assumed to be the settling velocity of the particles, which is estimated by the Rubey's equation.

The model has been developed by solving 3D Navier-Stokes equations with Boussinesq approximation and mass conservation equations using large eddy simulation (LES), and the modified Smagorinsky model⁴⁾ is used for turbulence closure. As solution methodology, using splitting approach, the governing equations are split into three parts, i.e., advection, diffusion and pressure part. The advection equations are solved by ULTIMATE QUICKEST⁹⁾. The diffusion part is solved by central difference scheme and pressure part is solved by successive over relaxation method.

The imposed boundary conditions for velocity, pressure and concentration are $U_1 = 0$, for bottom and side boundaries, $\partial U_1 / \partial x = 0$, $\partial U_3 / \partial z = 0$, and $U_2 = 0$, for top boundary, $\partial P / \partial x_i = 0$ and $\partial C / \partial x_i = 0$, for all boundaries. The free water surface is treated as a horizontal rigid boundary. An additional boundary condition is imposed to take the deposition of particles from the flow onto the bed into account. The net deposition rate D is estimated by $D = \alpha V_s C_b$, where α = a coefficient to be calibrated with experimental data, and C_b = near bed reference concentration. The fence is created in the simulations by taking no flow boundary condition i.e. $U_1 = 0$, $C = 0$, and $P = 0$ at the location of fence in the domain.

4. MODEL CONSTANTS

The computations are performed on a structured grid of size $\Delta x = \Delta y = \Delta z = 0.25M$ (2cm). The time step $\Delta t = 0.0025$ second. In order to determine the values of model constants, namely, Smagorinsky constant C_s , turbulent Schmidt number S_{ct} , and a coefficient α for the net deposition rate of sediments, simulations are carried out taking the data from 2D particle clouds experiments, which deals with the motion and diffusion of the clouds induced by direct dumping of sediments from the falling to spreading stage, reported by Akiyama et al.⁷⁾.

C_s and S_{ct} are quantified via the falling stage, and α is via spreading stage of the particle clouds. The distance measured from the water surface to the mass center of the cloud z , half width H , mass center velocity V and average effective gravity force B ($=W_0/A$) of the falling clouds and the effective gravity force of deposited particles W_d of the spreading clouds are non-dimensionalised as $z^* = z/A_0^{1/3}$, $H^* = H/A_0^{1/3}$, $V^* = V/((W_0^{1/2})/A_0^{1/3})$, $B^* = B/(W_0/A_0)$ and $W_d^* = W_d/W_0$ respectively. A is the area of the cloud at z . The value of C_s typically ranges from 0.07 to 0.27¹⁰⁾. From simulation runs, it was observed that on this grid resolution, H^* , V^* and

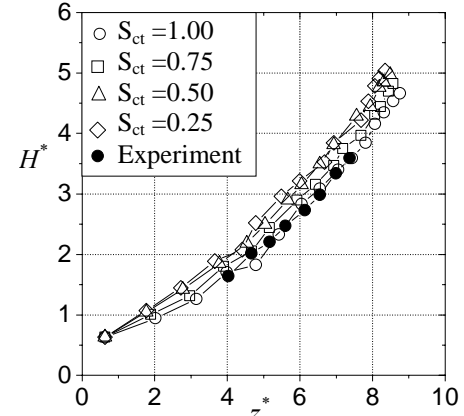


Fig.2 Sensitivity of S_{ct} on H^*

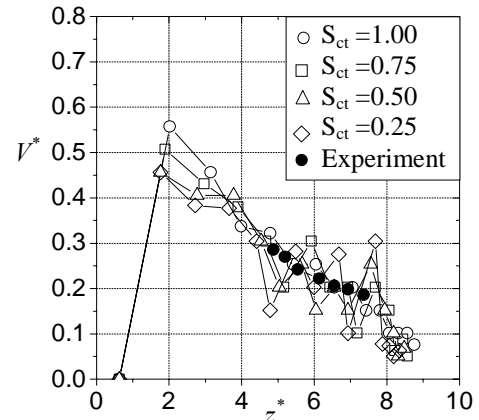


Fig.3 Sensitivity of S_{ct} on V^*

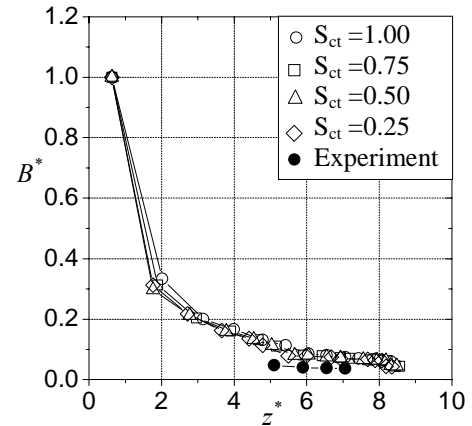


Fig.4 Sensitivity of S_{ct} on B^*

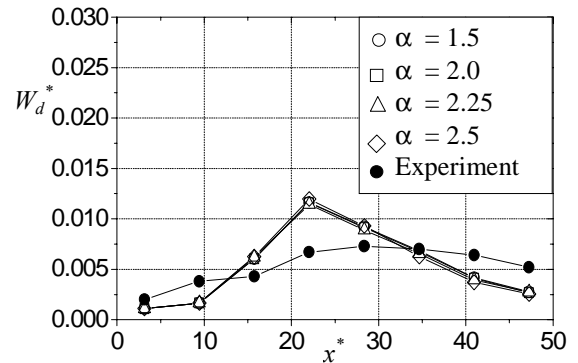


Fig.5 Sensitivity of α on W_d^*

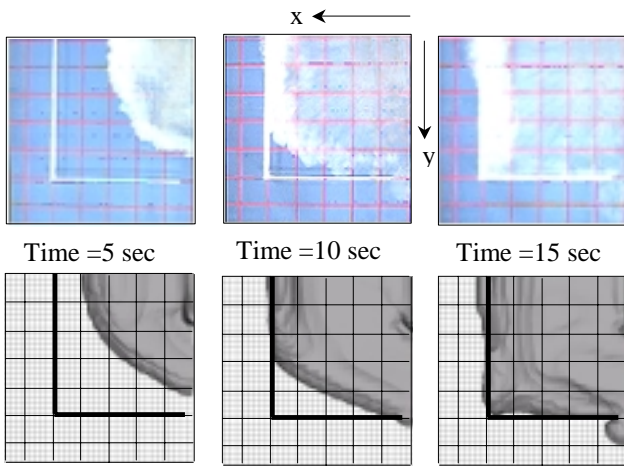


Fig.6 Spreading of the current for case 1. Experiment (above) and simulation (below)

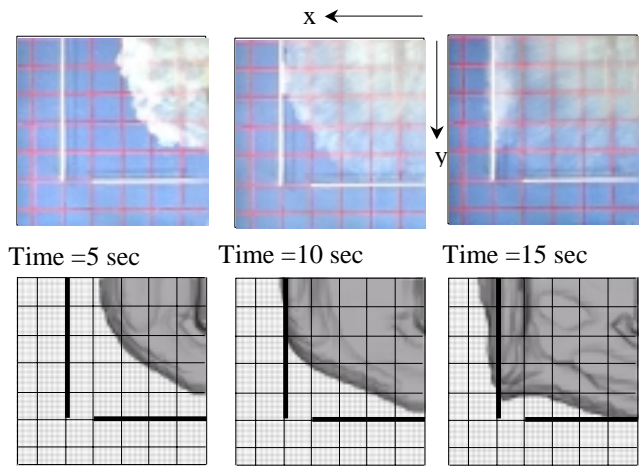


Fig.9 Spreading of the current for case 2. Experiment (above) and simulation (below)

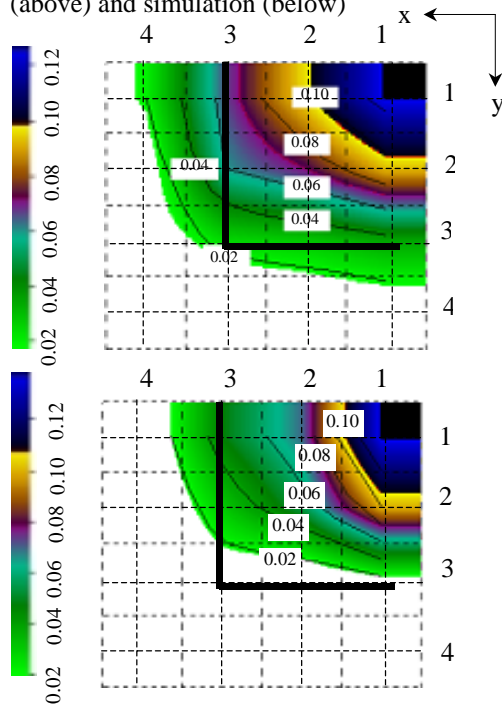


Fig. 7 Contours of W_d^* for case 1. Experiment (above) and simulated (below)

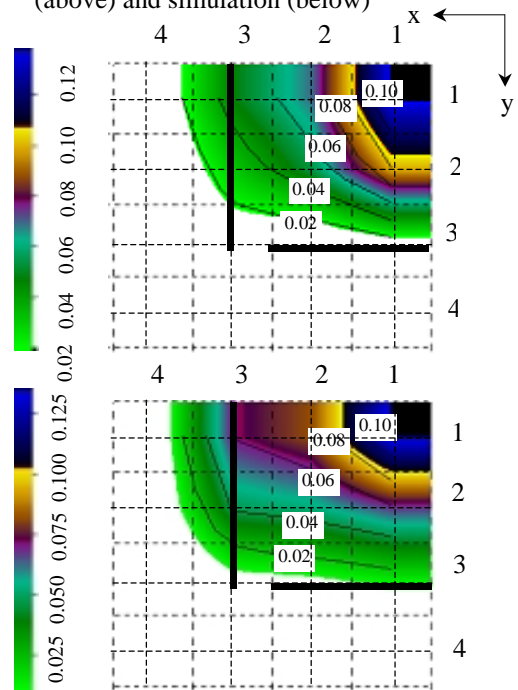


Fig.10 Contours of W_d^* for case 2. Experiment (above) and simulated (below)

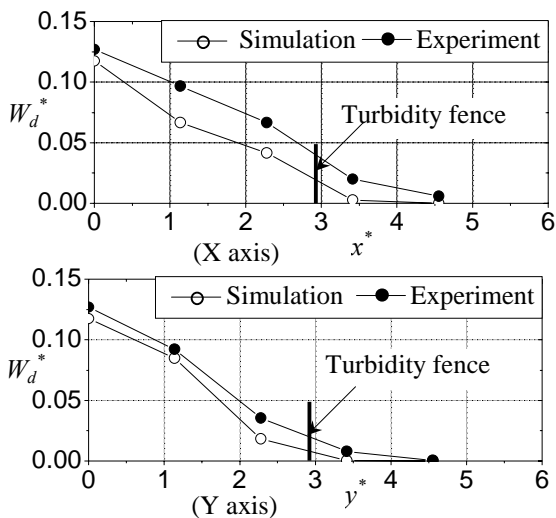


Fig. 8 W_d^* along the X axis (above) and the Y axis (below) for Case 1.

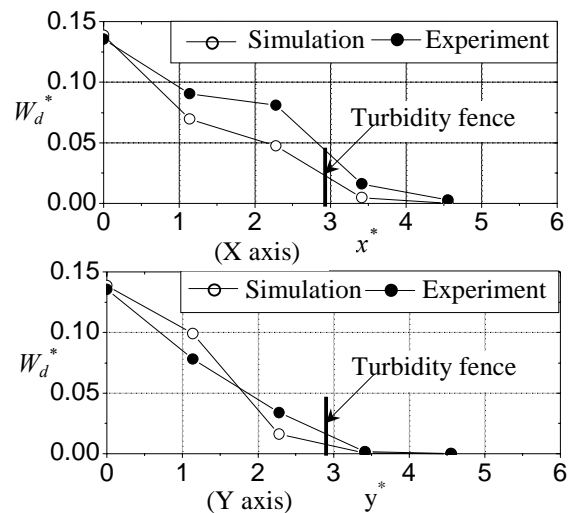


Fig.11 W_d^* along the X axis (above) and the Y axis (below) for Case 2.

Table 1. Conditions for numerical experiments

Case	Turbidity Fence	Fence height	Distance from suspension box
1	No fence	-----	-----
2	Fence	3/4 M	3/4 L
3	Fence	1/4 M	3/4 L
4	Fence	3/4 M	1/2 L

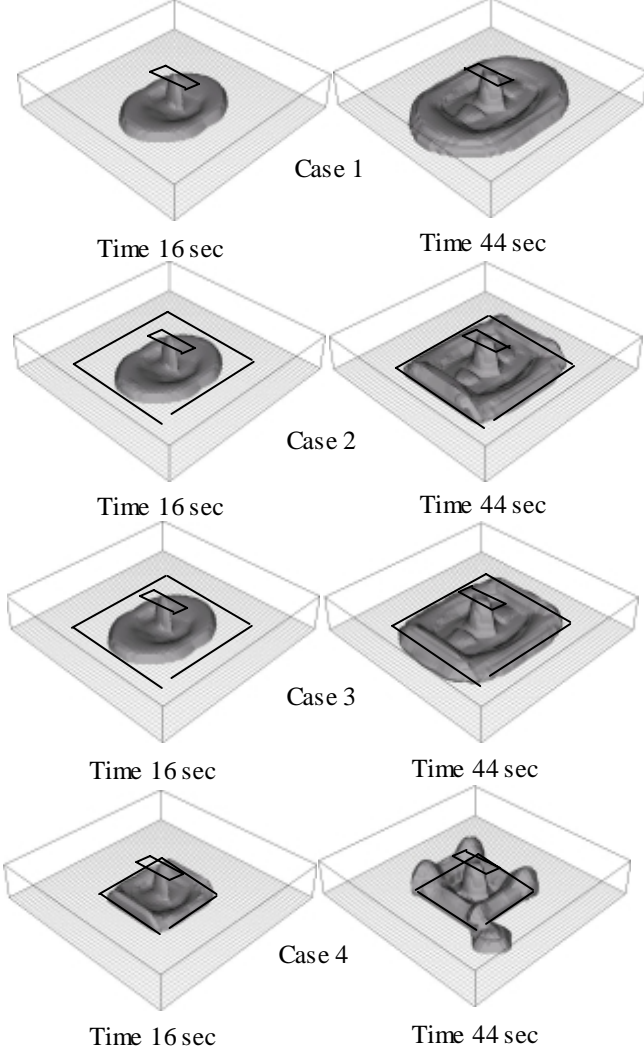


Fig. 12 Simulated currents under the different positions and height of the fence.

B^* are found insensitive to C_s , so that $C_s = 0.15$, which is reported by Ying et al.⁴⁾ and Akiyama et al.⁷⁾, is adapted. The value of S_{ct} is varied from 0.25 to 1.0. The sensitivity of S_{ct} to H^* , V^* and B^* is examined as shown in Figs.2~ 4, and $S_{ct} = 1.0$ is found to yield the closest match with the experimental results.

α is optimized taking $\alpha = 1.5, 2.0, 2.25$ and 2.5 . Fig.5 shows the comparison of simulated W_d^* with the experimental result of the spreading stage of 2D particle clouds. It is observed that W_d^* is almost insensitive to α , but $\alpha=2.25$ is found to be closest to the experimental result. In the following

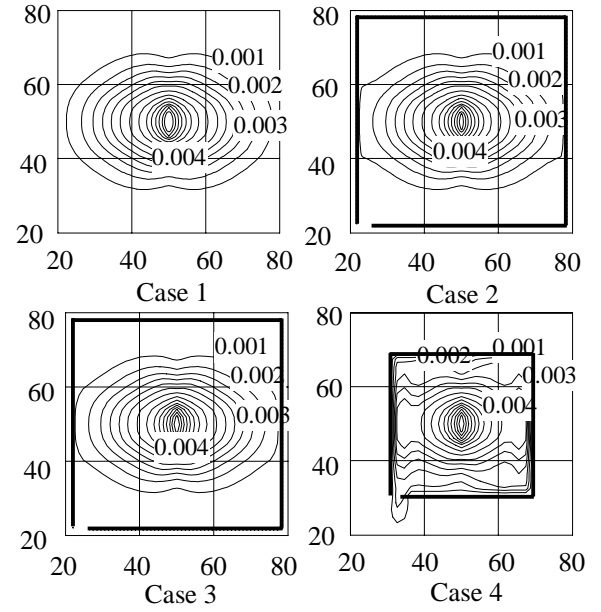


Fig. 13 Simulated contours of W_d^* under the different positions and height of fence.

computations, $C_s = 0.15$, $S_{ct} = 1.0$ and $\alpha = 2.25$ will be used.

5. RESULTS AND DISCUSSION

The computations are performed on cartesian grid of $200 \times 200 \times 25$ nodes. The initial suspension is defined on the bottom of the domain and occupies $4 \times 20 \times 8$ nodes. The analysis is carried out for the $1/4$ portion of the domain shown in Fig.1, because the identical results were observed in the rest.

Fig.6 shows the comparison of experimental photographs and simulated currents for Case 1. The square in the figure measures an area of $10 \times 10 \text{ cm}^2$. The shape and position of simulated currents at each time are in reasonable agreement with the experimental photographs. It is observed that the flow is more dominant along the X axis, owing to the effect of the aspect ratio, and that when the current reaches the fence, some of sediments overflow the fence and diffuses out of the fence.

Fig.7 shows the comparison of contours of simulated non-dimensional effective gravity force of deposited particles W_d^* ($=W_d/W_0$) with the experiments. x and y are the distances along the X axis and Y axis and are non-dimensionalised as $x^* = x/A_0^{1/3}$ and $y^* = y/A_0^{1/3}$, respectively. It is observed in simulations as well as experiments that the most of the sediments are deposited close to the source. W_d^* decreases with increase in distance from the source. The contours of simulated W_d^* are in reasonable agreement with the experiments.

Fig. 8 shows the comparison of the calculated profiles of W_d^* along both axis, i.e., X axis and Y axis, with the experimentally observed ones. It is

observed that the model underestimates W_d^* along the X axis, and reproduces W_d^* to a reasonable accuracy along the Y axis. The total amount of deposited sediments contained within the turbidity fence is about 90% of the initial total amount of sediments released in the experiments, whereas in the simulations about 93%.

Figs. 9~11 show the comparisons for Case 2. The matching between experimental and calculated results are identically reasonable as Case 1. In Case 2, as the opening is farther from the box, more time is required for the front to reach the opening and hence results in more deposition of particles. The total amount of deposited sediments within the fence is about 95% of the initial total amount of sediments, whereas in the simulations about 97%.

6. NUMERICAL EXPERIMENTS

Numerical experiments are conducted by changing positions and heights of the fence as shown in Table 1. The computational domain is $12.5M \times 12.5M \times 2.5M$. The suspension is introduced as $1 \times 5 \times 4$ nodes just below the surface of the domain. ϵ_0 is 0.0175. W_0 is $2747 \text{ cm}^4/\text{s}^2$.

Fig.12 and 13 respectively show the simulated results of the flow pattern and the contours of W_d^* . The followings is observed. The placement of fence is effective in reducing diffusion of turbidity. More turbidity is diffused out of the fence as the fence height lowers. Substantial amount of turbidity escapes from the opening in the corner when a higher fence is placed close to the dumping point. Most of the sediment is deposited near the dumping point. The distribution of sediments in the fence with lower height is almost similar to the case of no fence. The sediment deposited in areas under two different positions of fence placement in Case 1 are 98% and 88%, respectively. The sediment diffused out of the fence area for Case 2, 3 and 4 are identical 1%, 1.2% and 1.5% of the total sediments, respectively.

7. CONCLUSIONS

3D numerical simulations as well as newly obtained experimental data on 3D suspension gravity currents under the presence of a turbidity fence are presented. The following are findings and suggestions obtained from this study.

(1)The values of model constants are identified as $C_s = 0.15$, $S_{ct} = 1.0$ and $\alpha = 2.25$ by using the existing data of 2D suspension clouds although α may be need to express in terms of local flow conditions in order to reproduce the depositing mechanism of the currents.

(2)The model is found to be capable of reproducing the complex behaviors of 3D suspension gravity currents under the presence of a fence to a reasonable accuracy, and the amount of sediments contained within the fence to a good accuracy.

(3)Numerical experiments are conducted to demonstrate that the present model is a useful tool in optimizing the position of a fence to achieve a desired level of diffusion of turbidity induced by direct dumping of sediments into a body of water.

REFERENCES

- 1) Necker, F., Hartel, C. and Moiburg, E.: High-resolution simulations of particle-driven gravity currents, *International Journal of Multiphase Flow*, Vol.28 (2), pp. 279-300, 2002.
- 2) Akiyama, J., Shigeeda, M. and Maeda, Y.: Three-dimensional numerical simulations of suspension thermal on horizontal bed, *Annual Journal of Hydraulic Engineering*, JSCE, Vol.48, pp.1165-1170, 2004.
- 3) Huang, H., Imran, J. and Carlos, P.: Numerical model of turbidity currents with a deforming bottom boundary, *Journal of Hydraulic Engineering*, ASCE, Vol.131 (4), 2005.pp283-293.
- 4) Ying, X., Akiyama, J. and Ura, M.: Numerical investigation on 2-D particle clouds, *Annual Journal of Hydraulic Engineering*, JSCE, Vol.44, pp.1239-1244, 2000.
- 5) Li, C.W. and Zang, F.: Three-dimensional simulation of clouds using a split operator scheme, *International Journal of Numerical Methods in Heat and Fluid Flow*, Vol.6 (2), pp.23-25, 1996.
- 6) Singh, J., Akiyama, J. and Shigeeda, M.: Numerical simulation of axisymmetric gravity current induced by direct dumping of sediments, *Annual Journal of Hydraulic Engineering*, JSCE, Vol.49, pp.1399-1404, 2005.
- 7) Akiyama, J., Jha, A.K., Ying. X. and Ura, M.: Numerical study of 2-D particle clouds and effect of turbidity fences, *Journal of Hydrosciences and Hydraulic Engineering*, Vol.19 (1), pp.141-152, 2001.
- 8) Snider, D.M.: An incompressible three-dimensional multiphase particle-in-cell model for dense particle flows, *Journal of Computational Physics*, Vol.170, pp.523-549, 2001.
- 9) Leonard, B. P.: The ULTIMATE conservative difference scheme applied to unsteady one-dimensional advection, *Computer Methods in Applied Mechanics and Engineering*, Vol. 88, pp.17-74, 1991.
- 10) Murakami, S. and Iizuka, S.: CFD analysis of turbulent flows past square cylinder using dynamic LES, *Journal of Fluids and Structures*, Vol.13, pp.1097-1112, 1999.